MULTIPASS BEAM BREAKUP IN RECIRCULATING LINACS*

Joseph J. Bisognano, CEBAF, 12070 Jefferson Ave, Newport News, VA 23606
Robert L. Gluckstern, Physics Dept., Univ. of Maryland, College Park, MD 20742

ABSTRACT

Multipass beam breakup, a transverse beam instability generated by coherent excitation of cavity higher order modes in a recirculating linac, is a particular concern in designs utilizing superconducting technology. In this paper an analytic model is presented that includes a description of this effect for a distribution of cavities along the linac with several recirculations in an impulse approximation. For N passes and M cavities, solution of the resulting equations reduces in general to finding M zeros of a 2(N-1) dimensional determinant or equivalently the M eigenvalues of an M-dimensional matrix. The parametric dependence of this system on higher order mode frequencies and Q, lattice functions, and transit times is discussed. Numerical examples are presented to clarify these issues and to model the CEBAF superconducting linac, where threshold currents are found to exceed design currents by more than an order of magnitude.

INTRODUCTION

In the design of CW linear accelerators using the latest generation of superconducting RF cavities, cost optimization and certain operational requirements (e.g., multiple extracted beams) favor configurations where the beam passes several times through the same accelerating structure. It has long been recognized that recirculating a beam through a linac cavity can lead to a transverse instability in which transverse displacement on successive recirculations can excite modes that further deflect the initial beam. The recirculated beam and cavities form a feedback loop that can be driven unstable at sufficiently high currents, and this effect is worsened by the higher Q's associated with modes of a superconducting RF structure. This multipass beam breakup has limited the current of early superconducting linacs such as the Stanford recyclotron [1] to currents of a few tens of microamperes. However, as will be shown in the following, improvements obtained in HOM damping lead to significantly higher threshold currents.

Earlier work [2,3] has addressed this effect by calculating the beam trajectory in a single cavity. Given the lower HOM Q's obtained through external coupling of superconducting cavities of the latest design and estimates of cavity to cavity frequency variations, it is clear that many of the modes of the cavities distributed along the linac overlap in frequency. Analytic and numerical efforts [4,5] have addressed this problem with specific attention to the design of the CEBAF superconducting recirculating linac. In this paper some refinements and applications of this work are presented.

ANALYTIC MODEL

The difference equations in an impulse approximation for the transverse displacement and momentum on the pth traversal (p-1 recirculation), denoted by the two component vector U_p(n,M) for the Mth bunch at the entrance to the nth cavity, can be generalized from that for a single traversal [6] to obtain

$$U_p(n,\,M) = T^{pp}_{n,n-1}\;U_p\,(n-1,\,M) + I Z_{n-1} T^{pp}_{n,n-1} \times$$

$$G \sum_{r=1}^{n_p} \;\sum_{k=1}^{M+(p-r)M_o-1} U_r(n-1, M+(p-r)M_o - k)\, s_k\,(\omega_n \tau) \qquad (1)$$

where

$T^{pq}_{n,m}$ is the transfer matrix on (x, p_x)

$Z_n = \dfrac{Z''_n \ell e}{2Q f_b}$

$G = \binom{0\;0}{1\;0}$

Z''_n = transverse impedance of cavity/unit length

M_0 = number of bunches in one recirculation

ℓ = cavity length

$f_b = \dfrac{1}{\tau}$ = bunching frequency

$s_k(\omega_n\tau) = e^{-\frac{k\omega_n\tau}{2Q}} \sin(k\omega_n\tau)$

n_p = passes

n_o = number of cavity sites

I = average beam current

For the last site the transformation takes U_p(n_0,M) to U_{p+1}(1,M).

If we assume a steady state solution to equation (1) of the form

$$U_p(n, M) = e^{i\Omega M\tau}\; V_p(n) \qquad (2)$$

for M large, we obtain the set of equations

$$V_p(n) = T^{pp}_{n,n-1}\;\; V_p\;(n-1)$$

$$+ I\; Z_{n-1}\; T^{pp}_{n,n-1}\;\; G \sum_{r=1}^{n_p} e^{i(p-r)M_o\Omega\tau}\;\; h_n(\Omega) V_p(n-1)$$

$$\text{for n} > 1 \qquad (3a)$$

$$V_{p+1}(1) = T^{p+1\;p}_{1,n_o}\;\; V_p(n_o)\;\; +$$

$$I\; Z_{n_o}\;\; T^{p+1\;p}_{1,n_o}\;\; G \sum_{r=1}^{n_p} e^{i(p-r)M_o\Omega\tau}\;\; h_n(\Omega) V_p(n_o) \qquad (3b)$$

where

$$h_n(\Omega) = \frac{H_n(\Omega)\,\sin\,(\omega_n\tau)}{1 + H_n(\Omega)^2 - 2\,H_n(\Omega)\cos(\omega_n\tau)}$$

$$H_n(\Omega) = e^{-\frac{\omega_n\tau}{2Q}}\;\; e^{-i\Omega\tau}$$

Now we can proceed in two distinct directions in setting up the equation for numerical solution. First, note that the V_p(n+1) are expressed solely in terms of V_r(n) for n > 1, and the V_p(1) are expressed solely in terms of the V_r(n_0) where n_0 is the last cavity site. Thus, starting with equation (3b) and inserting first the expression for V_p(n_0) in terms of V_r(n_0-1) and so

*This work was supported by the U.S. Department of Energy under contracts DE-AC05-84ER4015 and DE-AS05-80ER10666.

on, we have a complicated, but low-dimension equation for $V_p(1)$ in terms of $V_r(1)$. Since the $V_1(1)$ terms represent initial conditions of the incoming beam, the resulting equation for coherent motion reduces to a 2(N-1) dimensional equation for an N-pass system; that is, coherent motion is obtained when the determinant of the underlying 2(N-1) matrix is zero. For a second point of view, note that the right hand side of equations (3a) and (3b) depend on the average value, $\bar{V}$, summed over pass number. Thus, this system can be summed to yield an equation for $\bar{V}(n)$ in terms of all $\bar{V}(m)$, described by a matrix of dimension $2n_0$. In fact, because of the G matrix, the underlying matrix is of dimension n_0. The resulting linear system of n_0 equations (for D_i, the x-component of $\bar{V}(i)$) is

$$D_i = I \sum_{p=2}^{n_p} \sum_{r<p} \sum_{\ell=1}^{n_o} \left(T_{i,\ell}^{pr}\right)_{12} e^{M_0 \Omega \tau\, (p-r)}\ Z_\ell\, h_\ell(\Omega) D_\ell$$

$$+I \sum_{p=1}^{n_p} \sum_{\ell=1}^{i-1} \left(T_{i,\ell}^{pp}\right)_{12} Z_\ell h_\ell(\Omega) D_\ell \qquad (4)$$

and is of the form of an eigenvalue equation with the inverse of the current as the eigenvalue. Thus, for fixed coherent frequency Ω there are in general n_0 complex currents.

NUMERICAL SEARCH FOR INSTABILITY THRESHOLDS

To find thresholds for instability one may search in frequency and current in various ways. For this study, a plot of complex current eigenvalues has been found useful. First, the coherent frequency is swept in real frequency with an arbitrarily small imaginary part corresponding to growth. The n_0 families of complex current eigenvalues are then determined, with the actual threshold current corresponding to the smallest positive real value obtained. Figure 1 illustrates the simplest such plot for a single cavity location in two passes. Figure 2 shows the added complexity for a four-pass configuration.

The spiraling of the figures is driven by the $\exp(i\Omega M_0\tau)$ factors together with the rolling-off of the impedance away from resonance. Although physically realizable currents correspond to the positive real axis, changes in resonator frequency or recirculation time delay can rotate the figure. Thus, the entire locus of points near the origin provides information about the threshold currents.

For higher-Q resonators the effects of frequency change on threshold current can be quite dramatic. Figures 3 and 4 illustrate this effect for a Q=320000 resonator with frequencies changed from 1890.75 to 1890.81 MHz with a recirculation path length of 4.19 microseconds. The threshold current differs roughly by a factor of 4. Note from Figures 1 and 2, going from 1 to 3 recirculations can have a comparable effect. Thus, when beam breakup is driven by individual cavities (as would be the case when HOM are not well damped) consistent prediction, except for worst case minimum currents, would be difficult.

The situation is clearly different for a set of overlapping resonators distributed along the linac. Figure 5 represents the threshold current for a modeling of the CEBAF recirculating linac by 50 "supercavity" modes (as discussed in reference [5]) corresponding to the strongest HOM with an estimated frequency spread of 1 MHz. A threshold current of approximately 12 mA is found. This result is in good agreement with more detailed computer simulation, which is reported in another paper at this conference [7]. The design current for CEBAF is 200 microamperes.

LATTICE OPTIMIZATION

As can be seen from equation (4), the threshold current depends on the lattice through the 1-2 matrix elements between all cavity sites on all passes. For a single cavity and one recirculation, therefore, absolute stability can be obtained by forcing the single 1-2 matrix element to zero. Consider now 2 cavity locations with the same resonator frequency. Figure 6 shows the two root families when the phase advance is chosen to be 0 (mod 360) degrees for site 1, and Figure 7 shows the two root families when the average of the phase advance for site 1 and site 2 is chosen to be 0 (mod 360) degrees. Clearly the second choice has obtained an at least local maximum in threshold current with improvement by about a factor of 2. Similar effects have been found for the three cavity site configuration. It would appear that care in the choice of recirculation phase advance can have a nontrivial impact on current limits, although nothing as singular as the single cavity case has been observed for a distribution of cavities. For a long, distributed linac such as CEBAF, a lattice with constant phase advance in the first pass is found to exhibit threshold currents higher by roughly a factor of 3 for multipass beam breakup than a lattice with constant magnet strength with the same phase advance in the first cell.

CONCLUSION

Analysis of multipass beam breakup is sufficiently well developed to provide an alternative to bunch by bunch simulations in determining threshold currents. In addition, it can provide good insight into sensitivity to parameters. The next step is application of the method to steady state conditions below threshold, both in analysis of beam transfer functions and in the determination of emittance degradation.

ACKNOWLEDGMENT

The authors wish to recognize the efforts of Geoffrey Krafft and Sharon Laubach in assisting in this work.

REFERENCES

[1] C. M. Lyneis, et al., NIM, 204, 269 (1983).
[2] A. M. Vetter, Stanford Tech. Note HEPL TN 80-2 (1980).
[3] H. Herminghaus and H. Euteneuer, NIM, 163, 299 (1979).
[4] R. L. Gluckstern, 1986 Linear Accelerator Conference Proceedings, SLAC 303, 543.
[5] Joseph J. Bisognano and Geoffrey A. Krafft, 1986 Linear Accelerator Conference Proceedings, SLAC 303, 452.
[6] Gluckstern, Cooper, and Channell, Particle Accelerators, 16, 125 (1985).
[7] G. Krafft and J. Bisognano (this conference).

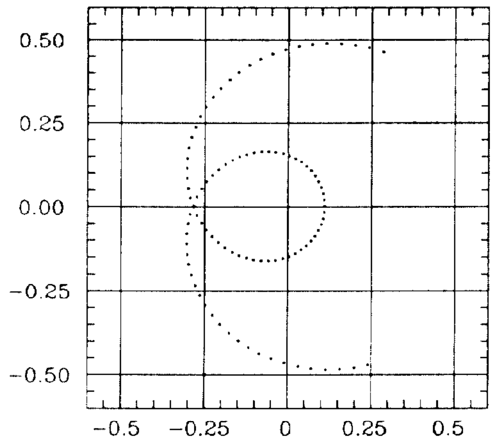

Figure 1
Stability plot of complex threshold current (amperes) for one site, two-pass configuration.

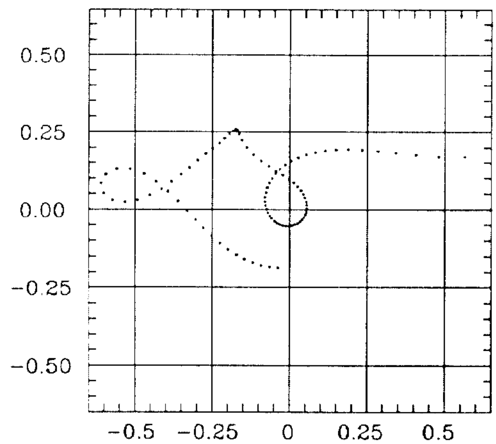

Figure 2
Stability plot of complex threshold current for one site, four-pass configuration.

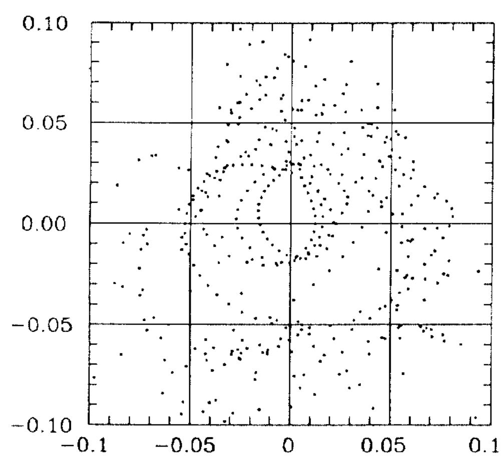

Figure 5
A model calculation of beam stability in the CEBAF recirculating linac (current in amperes).

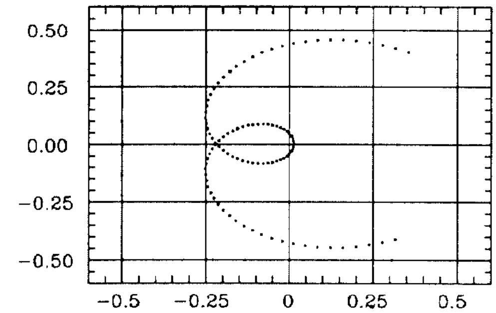

Figure 3
Stability plot for Q = 320000 resonator at 1890.75 MHz.

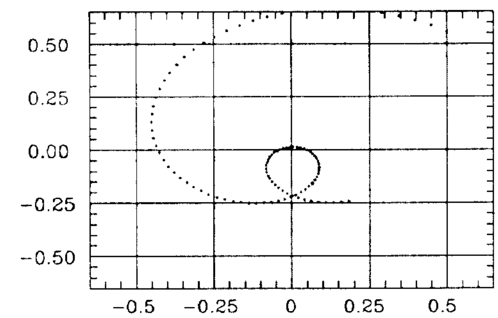

Figure 4
Stability plot for Q = 320000 resonator at 1890.81 MHz.

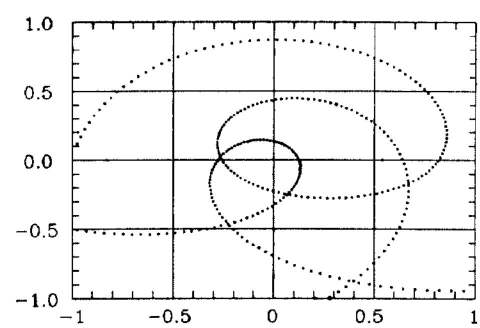

Figure 6
Stability plot for two cavity sites with 0 degrees from site 1, pass 1 to site 1 pass 2.

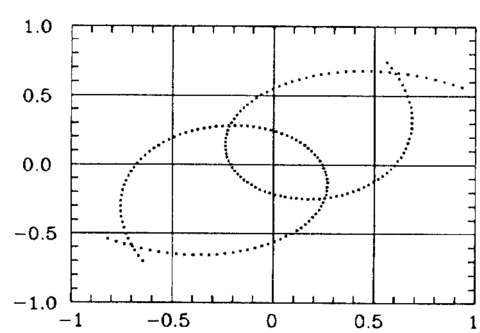

Figure 7
Stability plot for two cavity sites with 0 degrees phase advance for a location between site 1 and site 2 for pass 1 to pass 2.